Journal of the European Ceramic Society **19** (1999) 187–194

PII: S0955-2219(98)00191-5
0955-2219/98/$—see front matter

Carbothermal Synthesis of Vanadium and Chromium Carbides from Solution-Derived Precursors

H. Preiss,[a]* D. Schultze[b] and K. Szulzewsky[a]

[a]TU Bergakademie Freiberg, Institut für Energieverfahrenstechnik, Freiberg, Germany
[b]Bundesanstalt für Materialforschung und -prüfung (BAM), Berlin, Germany

(Received 22 April 1998; accepted 31 July 1998)

Abstract

Vanadium and chromium tartrate precursors prepared from aqueous solutions have been used as preceramic materials for carbothermal reactions with and without simultaneous nitridation. Their thermal behaviour has been investigated by TG/DTA, X-ray diffraction and measurement of surface areas. Under pyrolysis up to about 600°C, reactive composites consisting of intimately mixed carbon and amorphous M_2O_3 oxides are formed by salt decomposition. The subsequent processes of crystallization of oxides and carbothermal reduction render both the composites and the reduction products porous. The carbothermal reactions leading either to V_8C_7, a V(C,N,O) solid solution, and Cr_3C_2, respectively, proceed at moderate temperatures between 800 and 1100°C. The final products result as assemblages of fine carbide or carbonitride particles, however, with extensive heat treatment the particles grow and the surface areas diminish. Air oxidation of the final products has been studied by simultaneous TG/DTA. © *1998 Elsevier Science Limited. All rights reserved*

Keywords: calcination, porosity, carbides, catalysts, carbothermal reaction.

1 Introduction

Carbides and nitrides of the transition metals of the fourth to sixth group of the periodic table combine classical refractory properties with physical properties similar to those of metals. Interest in these physical properties, as electrical and thermal conductivity, Hall-coefficient, and magnetic susceptibility, has made these carbides promising candidates for heterogeneous catalysis. Hydroprocessing of hydrocarbon feedstocks by transition metal carbides and nitrides, including VC and VN, is one example for their use.[1] Unfortunately, the industrial preparation techniques starting mostly with metal oxides and solid carbon produce materials of very low specific surface area, not suitable as catalysts or catalyst supports. In order to exploit the advantages of these carbides, alternative techniques for the production of carbides with a high surface area have been developed recently.

CVD methods using organo-metallic precursors have been proved as widely practicable techniques for the production of carbide coatings and powders, also for vanadium[2] and chromium carbide[3] coatings. The very fine powders, however, are not usable for technical catalytical processes. Catalysts and catalyst supports have been produced by gas–solid reactions in which a flowing gas reacts with a solid. Thus, porous SiC and Mo_2C were obtained from porous carbon and vaporized metal oxides (SiO_2, MoO_2).[4] Porous carbon can also be impregnated by salt solutions. Succeeding heat treatment then forms porous materials with carbide coating.[5] Recently, submicron carbide particles were produced by the temperature-programmed carburization of oxide powders with CH_4/H_2 mixtures.[6] This method is usable for vanadium and chromium carbide, too. Pyrolysis of polymer-, sol–gel- or solution-derived precursors are some newer methods for synthesizing submicron carbide particles for ceramics. An important feature of precursor pyrolysis is the lowering of the carburization temperature because the reactants are intimately mixed, mostly on a molecular level. Examples for group VIb elements are the pyrolysis of chromium salicylate,[7] electrochemically prepared chromium

*To whom correspondence should be addressed at present address: Köllnische Straße 22a, 12439 Berlin, Germany.

polymer precursors[8] and solution-derived molybdenum and tungsten precursors.[9]

This paper describes a new process for the synthesis of vanadium and chromium carbides starting from precursors prepared in aqueous solutions. The solutions contain the transition metals and a pyrolyzable organic compound. In contrast to the very intensive work on aqueous phase routes to oxide ceramics, there are only few examples of synthetic approaches to non-oxide materials. Advantages of precursor preparation via aqueous solutions are that (1) a high homogeneity of reactants is achieved, (2) the required composition for the carbide formation can be adjusted by solution processes, and (3) no risky organic solvents are needed. Tartaric acid is used as the pyrolyzable organic compound. It forms coordination compounds with many inorganic cations. The succeeding thermal processes then include salt decomposition into an intimate mixture of metal oxide and carbon, and carbothermal reduction of the oxide.

Simultaneous thermogravimetric analysis (TG) and differential thermal analysis (DTA), as well as nitrogen adsorption measurement were used to follow the thermal processes. Phase identification was performed by X-ray diffraction (XRD) analysis. The final products were observed by scanning electron microscopy (SEM). Air oxidation of the final heating products was investigated with regard to their practical application.

2 Experimental Procedure

2.1 Sample preparation

In a solution of 6·20 g tartaric acid in 50 ml distilled water 1·82 g V_2O_5 (0·01 mol) (E. Merck) were suspended and dissolved to a clear solution by heating at ~60°C and stirring. During the dissolution process the color of the so obtained solution changed to blue and lastly to green, showing that reduction of V^{+5} to V^{+3} had taken place. The solution was then concentrated at ~60°C until a residue of a high viscosity had formed without any precipitation. Residual water was allowed to evaporate at room temperature and after that at 130°C. Thus, a precursor consisting of vanadium tartrate and free tartaric acid was obtained (exposure on open air partially reoxidizes V^{+3} to V^{+4}).

In 10 ml distilled water 1·00 g CrO_3 (0·01 mol) (E. Merck) was dissolved and dropwise added at 0°C to a solution of 3·35 g tartraric acid in 20 ml distilled water. Immediately with adding the solution of the chromic acid reduction of Cr^{+6} mostly to Cr^{+3} took place discernible by a warming of the mixed solution and a change of its color. The reduction reaction was finished when the color of the solution became violet. The violet solution contains a non-stoichiometric complex compound of chromium with tartaric acid. The solvent (water) was then partially evaporated at ~60°C until a gel-like residue had formed. Succeeding drying first at room temperature and lastly at 130°C led to a chromium tartrate precursor which was used for the thermal processes.

2.2 Heat treatment

The as-prepared precursors were annealed in graphite boats using an alumina tube furnace (Carbolite Furnace Limited) at 500–1500°C at 100°C intervals either in flowing argon or nitrogen. Nitrogen atmosphere was used to study the effect of simultaneous nitridation during the carbothermal reduction reaction. The heating rate was 10 $K\,min^{-1}$, and the holding time at the reaction temperature was 1 h.

2.3 Characterization

The thermal behaviour of the precursors in argon as well as in nitrogen atmosphere was studied up to 1265°C by simultaneous TG/DTA using a SETARAM TAG 24 thermoanalyser. The heating rate was 5 $K\,min^{-1}$. In order to check the completeness of the carbothermal reduction, the heating cycle was repeated after cooling the samples to room temperature under the appropriate atmosphere. Subsequently, TG/DTA was conducted in air for the final heating products to study their oxidation behaviour. The heating rate was 10 $K\,min^{-1}$ in these oxidation experiments.

Conventional X-ray diffractometry with nickel-filtered CuK_α radiation was used to determine the crystalline phases present in the heat-treated samples. BET surface areas were determined from nitrogen adsorption according to the method of Haul and Dümbgen[10] (simplified single point procedure).

Chemical analyses of the non-metals carbon and nitrogen were performed using a CHN-Analyser (EA 1110 of CE Instruments) designed for organic elemental analysis. Oxygen and nitrogen were additionally determined with LECO TC-436.

3 Results and Discussion

3.1 Thermal treatment of the vanadium precursor in argon

The thermal behaviour of the vanadium precursor in argon atmosphere was studied by simultaneous TG/DTA, X-ray diffraction and nitrogen adsorption measurement. The TG and DTA curves up to 1265°C (Fig. 1) can roughly be divided into four

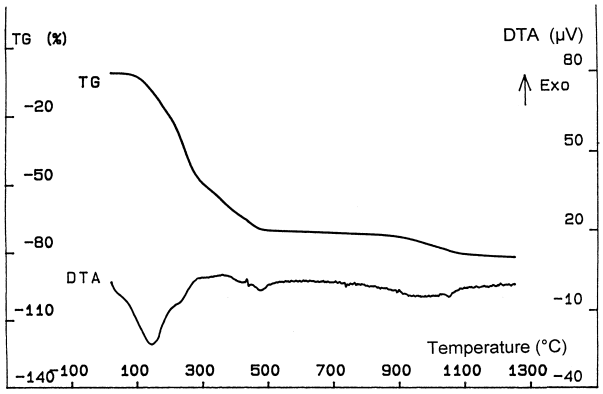

Fig. 1. TG/DTA diagram of the vanadium precursor measured under argon.

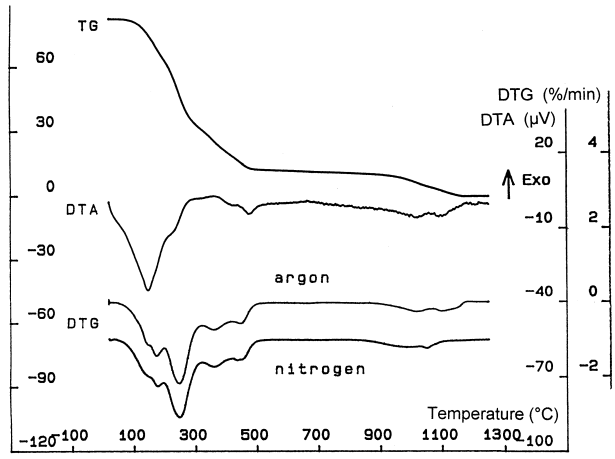

Fig. 2. TG/DTA diagram of the vanadium precursor measured under nitrogen; and differential thermogravic curves of the vanadium precursor measured under either argon or nitrogen.

sections: two regions of a considerable mass loss are followed by regions of nearly constant mass in each case. The first mass loss ranging from ~150 up to 500°C is mostly attributable to the decomposition of vanadium tartrate and tartaric acid whereby a pyrolysis coke is formed from the organic constituents. The DTA curve reveals endothermic peaks for these decomposition reactions with the exception of an exothermic peak between 260 and 420°C. Presumably, this exothermic peak is associative with the reduction of incompletely reduced or reoxidized vanadium species to V_2O_3. In the second region (~500–900°C), V_2O_3 and almost pure carbon are present in an intimately mixed composite material. Both TG and DTG curve show that no reactions besides crystallization take place. The crystallization of V_2O_3 in this temperature range (see below) proceeds without thermal effects.

The region of constant mass is followed by another mass loss caused by the release of CO during the carbothermal reduction reaction. According to the TG/DTA experiments, the onset of the carbothermal reduction is at 900°C, and its end point is at ~1170°C. A two-step mechanism for the carbothermal reduction is apparent from the DTA and DTG curves (Figs 1 and 2). Since the formation of oxycarbides preceding the carbothermal formation of the carbides of early transition metals—especially formation of cubic vanadium oxycarbide[11]—is widely known, the first reduction step may be attributable to the formation of an oxycarbide. Then, a conversion of the oxycarbide into vanadium carbide by a more or less complete substitution of oxygen by carbon can be assumed for the second step. Under this assumption, the intermediate after the first step arrived at ~1060°C should have a composition of $V(C_{>0.5}O_{<0.5})$ + free carbon. The substitution reaction seems to be almost finished at 1170°C because the mass is nearly constant in the fourth temperature region 1170–1265°C (mass loss 0·04 wt%). Such high degree of oxygen substitution by carbon at this moderate temperatures is surprising. It may be explained by the intimate mixture of the reactants in the precursor.

X-ray diffraction shows that the as-synthesized precursor is amorphous, and that it remains amorphous at heat treatment up to 600°C. At 700°C, broad lines of rhombohedral V_2O_3 are observable, indicating that the amorphous oxide has crystallized and has formed crystallites of nanometer size. With rising temperature these crystallites grow and the lines become narrower. Figure 3 depicts the XRD patterns of precursor samples annealed at 800, 900 and 1500°C. The pattern of

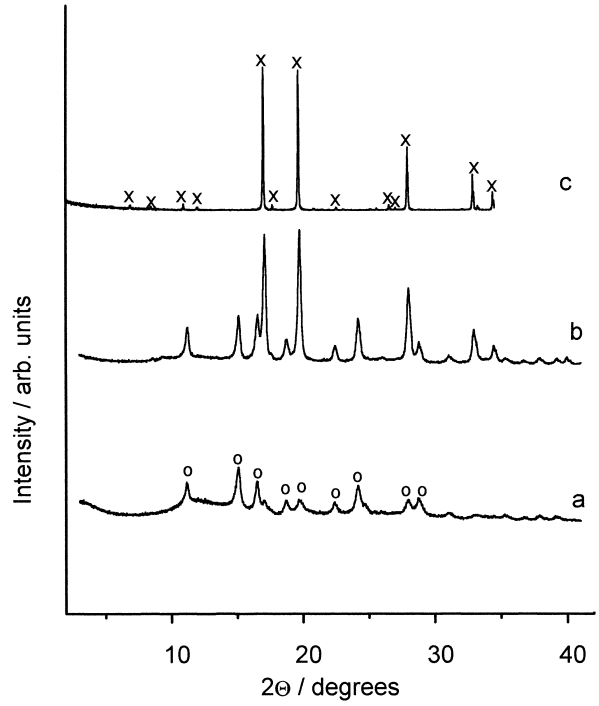

Fig. 3. X-ray diffraction patterns of the vanadium precursor annealed under argon at (a) 800°C, (b) 900°C and (c) 1500°C (o: V_2O_3; x: V_8C_7).

the 800°C sample is that of rhombohedral V_2O_3. At 900°C, strong lines attributable to a B1 rock salt type emerge in addition to the V_2O_3 lines. Presumably, these additional lines are those of cubic vanadium oxycarbide (JCPDS card 18-314) formed during the first reduction peak around 1000°C in the DTA experiment (Fig. 1). The shift to a lower temperature for the heating in the alumina furnace may be explained by the progress of the carburization reaction with time. Obviously, the annealing time of 1 h in the oven experiment enables more complete transformation of the oxide into the oxycarbide at 900°C. With further temperature increase the XRD-lines of V_2O_3 disappear, and the pattern becomes that of cubic V_8C_7 at 1200–1500°C [Fig. 3(c)]. The structure of this sub-carbide V_8C_7 is a superlattice structure of the general B1 rock salt type of the stoichiometric transition-metal monocarbides MC.[12] The lattice parameter is about twice that of the B1 substructure. The weak lines in Fig. 3(c) are indicative of ordering of the carbon atoms. The lattice parameter (a) determined from the pattern (Table 1) is very close to that reported (JCPDS card 35-786 for V_8C_7: $a = 8{\cdot}33409$ Å).

Table 1 also comprises results of the chemical analyses of the non-metals of the 1500°C sample. The carbon analysis shows that the final product contains 1–2 wt% non-bonded carbon (theoretical value for V_8C_7: 17·09 wt%). The low N amount may originate from nitrogen traces in the oven atmosphere. From the values for nitrogen and oxygen it can be inferred that only low portions of carbonitrides and oxycarbides are present.

3.2 Thermal treatment of the vanadium precursor under nitrogen

Figure 2 shows simultaneous TG/DTG/DTA curves for the heat treatment of the vanadium precursor in nitrogen atmosphere. Characteristic TG features are again two regions of strong mass loss attributable first to decomposition reactions and on the other hand to the carbothermal reduction. The DTA section, corresponding to the first mass loss (< 500°C), reveals two endothermic peaks which may be characteristic for the decomposition of the salt and free tartaric acid, and one additional exothermic peak (~260–420°C) which may be due to the completion of the reduction of vanadium species to V_2O_3. At about 500°C, pyrolysis of the organic material is nearly finished and mass remains constant up to the onset of the carbothermal reduction. The effect of simultaneous nitridation can be demonstrated by comparing the differential thermogravimetric (DTG) curves for the heat treatment under argon and nitrogen (Fig. 2). Both DTG curves are nearly identical up to about 800°C. The first major deviation is that the mass loss step of the carbothermal reduction in nitrogen is shifted to lower temperature in comparison to the treatment in an inert atmosphere. The onset of the reduction in nitrogen is at ~850°C, and its closure at 1110°C. Furthermore, neither the DTA curve nor the DTG curve in nitrogen (Fig. 2) exhibit a distinct split into two steps. Lastly, a noticeable mass loss is also stated above 1110°C (1·1 wt% up to 1265°C). These findings can be explained by a one-step mechanism of the carbothermal reduction with simultaneous nitridation leading to a solid solution V(C,N,O) at lower temperature than the reduction without nitridation. The further substitution of N and O by C is a time-consuming diffusion-controlled process ranging up to high temperatures (> 1110°C).

X-ray diffraction shows that the precursor is amorphous up to 600°C, and V_2O_3 begins to crystallize between 700 and 800°C. At 900°C, lines of a cubic B1 structure begin to appear which may be attributable to a solid solution V(C,N,O). Rising temperature renders the intensifies of the V_2O_3 lines smaller until only the lines of the cubic B1 structure are present at 1100–1300°C. The lattice parameter of this cubic V(C,N,O) determined from this pattern is $a = 4{\cdot}15349$ Å. This lattice parameter is greater than that for VN (JCPDS 35-768: $a = 4{\cdot}13916$ Å) and lower than the half value for V_8C_7 (JCPDS 35-786: $a/2$; 4·16704 Å) as expected for a solid solution V(C,N,O).

Recently, nitrogen adsorption has been proved to be a useful technique to follow the carbothermal formation of ZrC,[13] NbC and TaC[14] from gel precursors. It has been shown that the phenomena of crystallization, reduction and sintering control the porosity and surface area in the precursors and heating products. Therefore, BET surface areas have also been determined for the annealed vanadium precursors. Figure 4 shows the BET values for the precursors annealed at different temperatures under argon as well as under nitrogen. It is thought that the high BET values are indicative of porosity generated under heating both in argon and nitrogen atmosphere. Crystallization of V_2O_3 and its carbothermal reduction are the most probable processes which render the materials porous.

Table 1. Lattice parameters (a) and chemical analyses of non-metals of the final products of the vanadium precursors annealed under argon at 1500°C (V_8C_7) and under nitrogen at 1300°C [V(C,N,O)]

	a (Å)	C_{total} (wt%)	Nitrogen (wt%)	Oxygen (wt%)
V_8C_7	8·33336	18·3	0·3	0·9
V(C,N,O)	4·15349	19·3	14·2	4·8

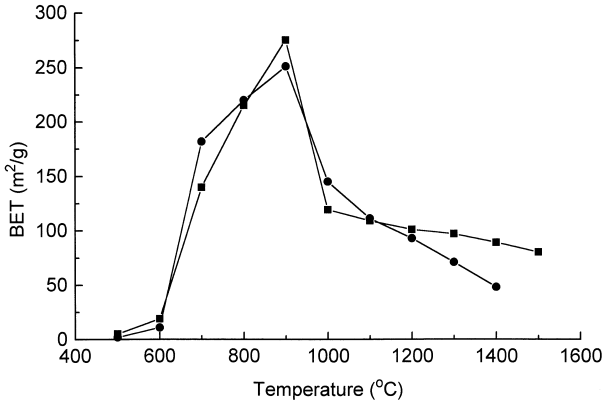

Fig. 4. BET surface areas of the vanadium precursor annealed under argon (■) and nitrogen (●).

Crystallization and reduction proceed in a narrow temperature range; the BET values are jointly corresponding for the annealing in argon and nitrogen up to 1000°C. The highest BET values at 900°C reflect a maximum of the reduction kinetics at this temperature (temperature differences in comparison with TG/DTA experiments are explained with the time-dependence of the reaction, see Section 3.1). Differences of the BET values for argon and nitrogen annealing are observable above 1100°C: the specific surface areas for nitrogen annealing are stronger reduced with rising temperature. Obviously, the solid solution V(C,N,O) formed this way sinters more than the carbide V_8C_7. The reasons for these different sintering phenomena are not yet clear.

3.3 Thermal treatment of the chromium precursor under argon

The chromium precursor was annealed only in argon atmosphere because intersolubility between the binary chromium nitrides and carbides is incomplete; the crystal structures of the nitrides and carbides are very different. Figure 5 shows simultaneous TG/DTA curves for the heating under argon up to 1265°C. Two sections of intensive mass loss and succeeding sections of nearly constant mass are observed. The first mass loss at 150–550°C is due for the first part to the decomposition of the chromium tartrate complex. Two endothermic DTA peaks centred at about 200 and 500°C are associative with this decomposition reaction. On the other hand, the completion of the reduction of some chromium species to Cr_2O_3 gives rise to additional mass loss and an exothermic DTA peak between 300 and 450°C. From 550 up to 860°C, mass is nearly constant and a composite has been formed, which is composed of Cr_2O_3 and carbon with a little excess of carbon (< 1 wt%) beyond that needed for the carburization reaction. The TG and DTA curves reveal the onset of the reduction reaction at 860°C and a sharp closing point for the reduction at 1075°C. No mass loss was observed during further temperature increase. A repeated heating cycle did also not show any additional mass loss. These findings and the overall mass loss are indicative of the formation of Cr_3C_2 without the intermediate formation of an oxycarbide.

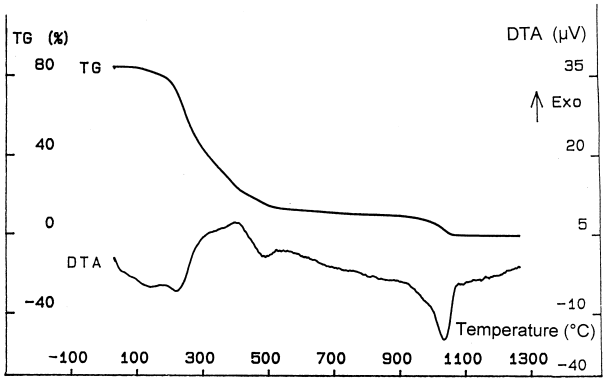

Fig. 5. TG/DTA diagram of the chromium precursor measured under argon.

Examination of the reaction sequence by XRD showed that the precursor as received after drying is X-ray amorphous. Crystallization of Cr_2O_3 in the precursor material begins during thermal treatment in the range 600–700°C. This is remarkably higher than the formation temperature of crystalline Cr_2O_3 from an oxide gel (400–500°C).[15] Figure 6 depicts the patterns of samples annealed at 800, 900 and 1000°C. The XRD pattern of the 800°C sample is that of rhombohedral Cr_2O_3. At

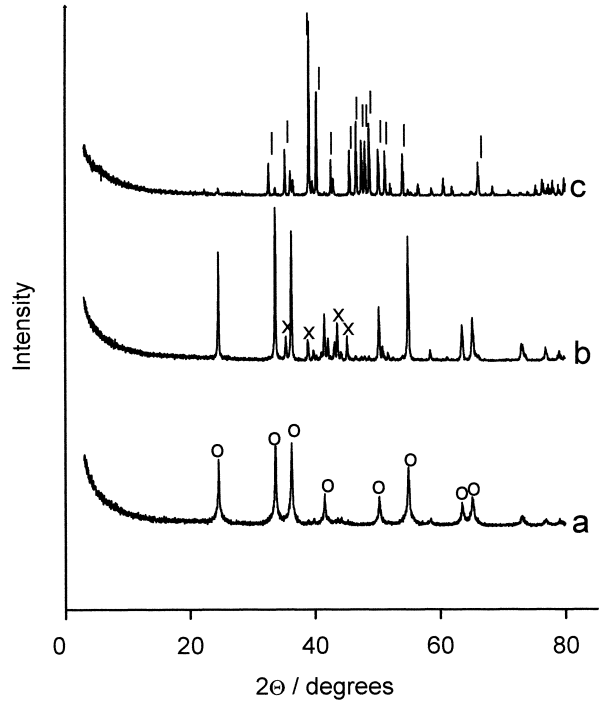

Fig. 6. X-ray diffraction patterns of the chromium precursor annealed under argon at (a) 800°C, (b) 900°C and (c) 1000°C (o: Cr_2O_3; x: Cr_3C_{2-x}; I: Cr_3C_2).

900°C, in addition to the Cr_2O_3 lines, some new lines appear which can be assigned to a metastable chromium carbide phase with a stoichiometry recently reported as Cr_3C_{2-x}, with a filled Re_3B structure.[16]

This metastable carbide formed from the tartrate precursor can transform during heating into the orthorhombic Cr_3C_2 (JCPDS card 35-804) by incorporation of carbon atoms. Figure 6 shows that this transformation is complete at 1000°C. Chemical analysis gives a carbon content of the final product at 1300°C of 13·5 wt% which is close to the theoretical value of Cr_3C_2 (13·3 wt%). Summarizing the XRD results the carbothermal reduction sequence in the precursor can be written as a successive reaction:

$$Cr_2O_3 \rightarrow Cr_3C_{2-x} \rightarrow Cr_3C_2$$

The BET values in Fig. 7 show that the precursor becomes porous at 600–700°C. The surface area increases with temperature in parallel to the crystallization of Cr_2O_3 and reaches a maximum at a temperature of 800°C before the carbothermal reduction starts. The carbide formation is connected with a striking decrease of surface area between 900 and 1000°C caused by sintering phenomena.

SEM micrographs taken from V_8C_7 and Cr_3C_2 demonstrate different high temperature agglomerization and sintering behaviour of both carbides (Fig. 8). The surface of a part of the vanadium precursor annealed at 1200°C shows a flat, broken structure consisting of agglomerated individual grains. Voids of a wide range of sizes between the grains are formed by the agglomerization process. These voids are suggested to be the entrances to pore systems. The micrograph of Cr_3C_2 produced at the same temperature, however, typically shows the phenomena of sintering. The particles are bond together by sintering, and they are still round in shape. The bigger particles and voids between them can explain the lower specific surface area already at this temperature in comparison to the vanadium carbide.

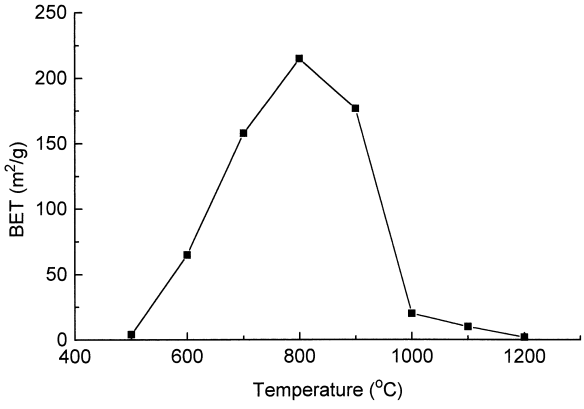

Fig. 7. BET surface areas of the chromium precursor annealed under argon.

3.4 Air oxidation

Oxidation reactions were performed in an air flow up to 610°C for V_8C_7 and V(C,N,O) and 1050°C for Cr_3C_2 with a holding time of 2 h at the maximum temperature in each case. The temperature of 610°C for the vanadium products has been choosen to avoid corrosion of the alumina crucibles by melting V_2O_5. Changes in color after oxidation confirmed that the final products are constituted of orange V_2O_5 and dark-green Cr_2O_3, respectively. The TG and DTA curves obtained for V_8C_7 and V(C,N,O) are depicted in Fig. 9(a) and (b). Only the TG curve of V_8C_7 shows a small mass loss immediately after the beginning of heating which is probably caused by the desorption of water entrapped upon opening the thermobalance before the oxidation run. These findings are concordant with the higher porosity of V_8C_7 in comparison with V(C,N,O) (see Fig. 4). Oxidation, discernible by mass increase of both compounds, begins at the

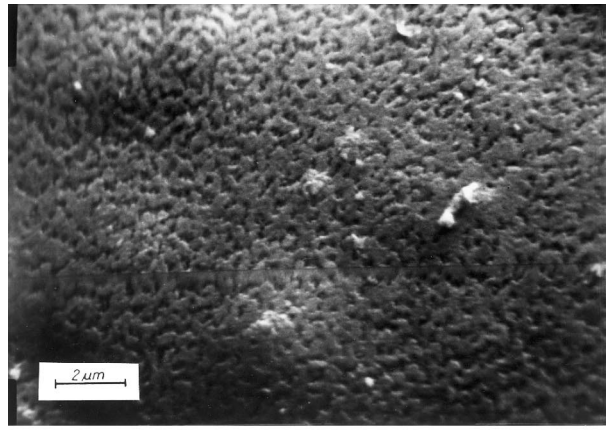

(a)

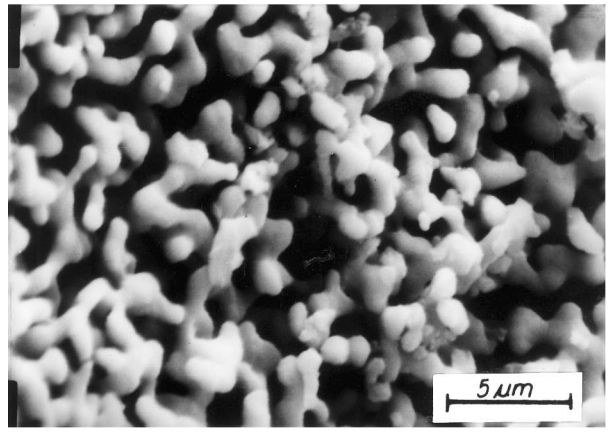

(b)

Fig. 8. Scanning electron micrographs of (a) V_8C_7 and (b) Cr_3C_2, both produced at 1200°C.

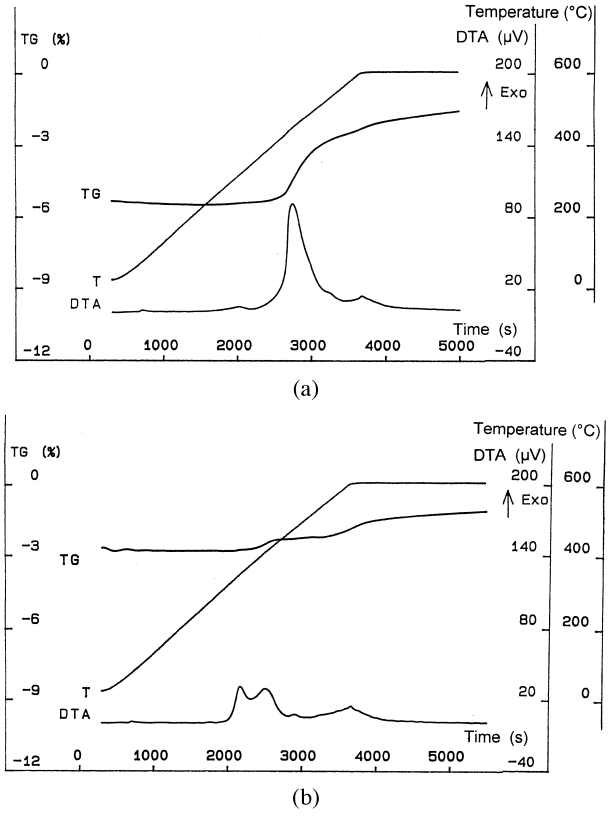

Fig. 9. TG/DTA diagrams of the oxidation in an air flow up to $T = 610°C$ of (a) V_8C_7 and (b) V(C,N,O), both produced at 1265°C.

same temperature (~180°C) and passes with rising temperature through three exothermic steps (A,B,C). The DTA curves reveal a higher intensity for V(C,N,O) during the step A (180–360°C) than for V_8C_7, however, opposite intensifies are found for both compounds during step B (360–500°C). Consequently, it is concluded that step A is due to the oxidative elimination of nitrogen in the compounds (according to the chemical analysis only a small byproduct of nitride is present in the precursor annealed under argon, see Section 3.1). Step B, however, may be associative with the maximum of the oxidation of bonded carbon. Step C may be explained by the transition to the section of constant temperature during the heating cycle. Throughout the temperature increase the reaction rate of the oxidation and, consequently, the DTA signal increase but during constant temperature the DTA signal decreases because of the consumption of the educts, V_8C_7 and V(C,N,O), respectively.

Figure 10 shows simultaneous TG/DTA oxidation curves of Cr_3C_2 obtained after two times repeated heating up to 1265°C under argon. In comparison with V_8C_7 the higher resistance against oxidation of the Cr_3C_2 is evident. The curves in Fig. 10 reveal the onset of the exothermal signal at ~530°C, however, mass increase starts at ~550°C and ends at ~1000°C. The presence of ~0·4 wt% of free carbon is estimated from the total mass

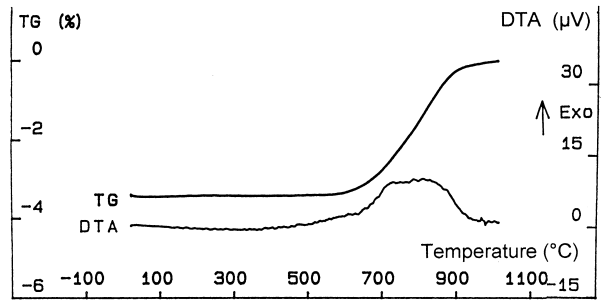

Fig. 10. TG/DTA diagram of the oxidation in an air flow of Cr_3C_2 produced at 1265°C.

increase up to 1000°C. It is thought that the burn-off of this free carbon coincides with the oxidation start of Cr_3C_2 and effects the shift of the onset of the exothermal signal to somewhat lower temperature in comparison to the onset of the TG signal. The DTA and DTG curves indicate that the overall oxidation obviously would proceed through several overlapping steps. It has been shown that Cr_3C_2 oxidizes in three steps[17] or in four steps[18] if it is exposed to air at a heating rate of $1\,K\,min^{-1}$. Presumably, distinct steps were not detected in the present work because of the faster heating rate.

4 Conclusions

The present work demonstrates that precursors for the synthesis of vanadium and chromium carbides can be prepared from aqueous solutions which contain tartaric acid and the respective cations. The solution route ensures an intimate mixing of the starting compounds, and additionally, reduction reactions proceed already in the solution stage. Salt decomposition leads to porous composites consisting of a homogeneous mixture of reactive carbon and finely divided V_2O_3 and Cr_2O_3, respectively. The use of precursor compounds instead of physical mixtures of the reactants is beneficial for the carbothermal carbide synthesis because it allows to work at moderate temperatures of 900–1000°C.

The solution routes offer a lot of advantages for synthesis reactions. The pyrolysis products obtained immediately after salt decomposition, the porous mixtures C/V_2O_3 and C/Cr_2O_3, are promising candidates for heterogeneous catalysis. An investigation of the aromatization of alkanes by C/Cr_2O_3 is currently in progress. Another advantage of practical use of the precursors is that the costs for the energy intensive carbide syntheses can be reduced. The fine grain carbide powders obtained may be used in ceramics. Additionally, the solution routes offer novel possibilities for the synthesis of ternary carbides and solid solutions.

Acknowledgements

The authors wish to thank Dr E. Schierhorn (BAM) for contributions to SEM observation.

References

1. Ramanathan, S. and Oyama, S. T., New catalysts for hydroprocessing: transition metal carbides and nitrides. *J. Phys. Chem.*, 1995, **99**, 16365–16372.
2. Cassoux, P., Choukroun, R., Cyr-Athis, O., Feurer, R., Laurent, F., Morancho, R., Theyssandier, F. and Valade, F., Molecular precursors for OMCVD preparation of TiN, VN, TiC and VC thin film ceramic materials. *Trans. Mater. Res. Soc. Jpn*, 1994, **19A**, 185–188.
3. Healy, M. D., Smith, D. C., Rubiano, R. R., Springer, R. W. and Parmeter, L. E., The organo-metallic vapor deposition of transition metal carbides: the use of homoleptic alkyles. *Mater. Res. Soc. Symp. Proc.*, 1994, **327**, 127–132.
4. Ledoux, M. J. and Pham-Huu, C., High specific surface area carbides of silicon and transition metals for catalysis. *Catal. Today*, 1992, **15**, 263–284.
5. Iwatani, S., Masumura, H., Sato, S. Taguchi, H. and Abe, H., Porous bodies and their manufacture. Japan Patent No. 06116055, 1994.
6. Oyama, S. T., Schlatter, J. C., Metcalf, J. E. and Lambert, J. M., Preparation and characterization of early transition-metal carbides and nitrides. *Ind. Eng. Chem. Res.*, 1988, **27**, 1639–1648.
7. Greco, C. C., Gallo, T. A. and Sherif, F. G., Manufacture of group VIB metal carbides from metal salicylate precursors. US Patent No. 5246685, 1993.
8. Rüssel, C., A pyrolytic route for the preparation of chromium carbide and chromium nitride. *J. Mater. Sci. Lett.*, 1992, **11**, 774–776.
9. Preiss, H., Meyer, B. and Olschewski, C., Preparation of molybdenum and tungsten carbides from solution derived precursors. *J. Mater. Sci.*, 1998, **33**, 713–722.
10. Haul, R. and Dümbgen, G., Vereinfachte Methode zur Messung von Oberflächengrößen durch Gasadsorption. *Chem. -Ing. -Tech.*, 1963, **35**, 586–589.
11. Gurevich, M. A. and Ormont, B. F., Investigation of phase relationship, structure and limits of homogeneity of the phase system V–C–O. *Zh. Neorgan. Khim.*, 1958, **3**, 403–412.
12. De Novion, C. H., Lorenzelli, R. and Costa, B., Superlattice structure in vanadium carbide VC_{1-x}. *C. R. Acad. Sci. Paris, Ser. B.*, 1966, **263B**, 775–778.
13. Preiss, H., Berger, L.-M. and Szulzewsky, K., Thermal treatment of binary carbonaceous/zirconia gels and formation of Zr(C,O,N) solid solutions. *Carbon*, 1996, **34**, 109–119.
14. Preiss, H., Schultze, D. and Klobes, P., Formation of NbC and TaC from gel-derived precursors. *Journal of the European Ceramic Society*, 1997, **17**, 1423–1435.
15. Carruthers, J. D. and Sing, K. S. W., Surface properties of calcined chromium oxide gel. *Chem. Ind.*, 1967, 1919–1920.
16. Bouzy, E., Bauer-Grosse, E. and Le Caer, G., NaCl and Re_3B-type structures for two metastable chromium carbides. *Philos. Mag. B*, 1993, **68**, 619–638.
17. Korablev, S. F., Lysenko, A. V. and Filipchenko, S. I., Chemistry and kinetics of the oxidation of powdered chromium carbide. *Poroshk. Metall. (Kiev)*, 1988, **7**, 88–92.
18. Loubiere, S., Laurent, Ch., Bonino, J. P. and Rousset, A., Elaboration, microstructure and reactivity of Cr_3C_2 powders of different morphology. *Mater. Res. Bull.*, 1995, **30**, 1535–1546.